

# Supporting information

## 1 TM5-GFEDV3 Comparison to MOPITT V5

We use version 5 of the MOPITT thermal infrared (TIR) level 2 product. MOPITT is a gas-filter correlation radiometer on board the Terra satellite that measures thermal emission near 4.7  $\mu\text{m}$  at a resolution of 22 km x 22 km. The local equator crossing time is 10:30/22:30, and global coverage is achieved in 3 days. CO vertical profiles of volume mixing ratio on a fixed pressure grid are retrieved with an optimal estimation technique (Deeter et al., 2010; Rodgers, 2000) for cloud-free scenes. A monthly climatology of the MOZART model provides the a priori vertical profile. The MOPITT instrument has the highest vertical sensitivity in the mid-troposphere, but also provides some boundary layer information (Deeter et al., 2007; Kar et al., 2008). As the Degrees of Freedom for signal is typically 1.5 (Deeter et al., 2004), we use the measured CO total column derived by integrating the CO vertical profile. Validation of version 5 data with respect to NOAA aircraft in situ CO profiles shows a mean bias of  $0.06 \times 10^{18}$  molecules/cm<sup>2</sup> with no clear geographical or time dependencies in the bias (Deeter et al., 2013; Worden et al., 2013).

As nighttime observations are less accurate (Yurganov et al., 2010), nighttime data were rejected. We only selected retrievals with  $\text{DFS} > 1.0$  to minimize the influence of the a priori. Finally, a first order correction for the geolocation bias was made by following the latitude/longitude bias correction recommendations in Table 1 of the MOPITT geolocation bias documentation (<http://web3.acd.ucar.edu/mopitt/GeolocationBiasReport.pdf>).

The satellite observations were gridded to  $1^\circ \times 1^\circ$ , where grid cell averages were taken only when MOPITT had enough valid observations to fill 30% of the grid cell. Following the recommendations in (Deeter et al., 2011), the MOPITT data were weighted by the Observation Quality Index (OQI; see the MOPITT v5 Users Guide [http://www.acd.ucar.edu/mopitt/v5\\_users\\_guide\\_beta.pdf](http://www.acd.ucar.edu/mopitt/v5_users_guide_beta.pdf)) during averaging to give more weight to observations with less geophysical noise.

## 2 Discussion of Uncertainties and Biases

In the following text we give an overview of recent model improvement and sensitivity studies, which gives some insight into possible biases in the TM5 v3 simulation and the DOMINO v2 NO<sub>2</sub> tropospheric column retrievals.

### 2.1 TM5 Chemistry

In (Williams et al., 2012) the authors implemented an on-line photolysis algorithm in TM5 v3 and found that a revised JNO<sub>2</sub> value increased NO<sub>2</sub> concentrations above 800 hpa, adding approximately  $0.2 \times 10^{15}$  molecules/cm<sup>2</sup> to the column over South America. Williams et al. (2012) also estimated that OH concentrations near the surface should increased by 15%, implying that the rate of conversion of NO<sub>2</sub> to HNO<sub>3</sub> via reaction with OH is biased low and the lifetime of NO<sub>x</sub> is overestimated in TM5 v3.

However, recent laboratory (Mollner et al., 2010) and aircraft (Henderson et al., 2012) observations indicate that the Sander et al. (2006) rate constant for this reaction, widely used in global chemical transport models, could be biased high by approximately 15-20%. Therefore, in the current configuration of TM5 v3, these two biases would largely offset each other, leaving a 5-10% high bias in the loss of NO<sub>2</sub> to HNO<sub>3</sub>, the predominant chemical sink of NO<sub>2</sub>, and therefore a high bias in  $\beta$ .

Because HO<sub>2</sub> loss to aerosols, a very uncertain but potentially important HO<sub>x</sub> sink, is not included in TM5 v3 the high bias in  $\beta$  for grid cells effected by biomass burning is likely greater than 5-10%. We therefore make an estimate based on the discussion above and the sensitivity simulations by (Stavrakou et al., 2013) of increasing the reaction probability of HO<sub>2</sub> uptake on aerosols to 1, that  $\beta$  is overestimated by 25% and that NO<sub>2</sub> tropospheric columns are biased low in TM5 v3 by  $0.2 \times 10^{15}$  molecules/cm<sup>2</sup> + 0-20%. This estimate is conservative as HO<sub>2</sub> uptake on aerosols equal to 1 is an upper limit for metal-doped aerosols.

## 2.2 Model Resolution and Sampling Errors

If the resolution of a  $\text{NO}_x$  emission source is significantly smaller than the resolution of the chemistry transport model, biases can occur in the estimate of  $\text{NO}_x$  emissions from model simulations because emissions from the point source will be artificially diluted to the coarse resolution model grid cell (Valin et al., 2011; Vinken et al., 2011). This dilution effect leads to errors in model  $\text{NO}_2$  concentration and  $\text{NO}_x$  lifetime.

This issue is most relevant for the estimate of  $\text{NO}_x$  emissions from fires in July, when burning is more spatially heterogeneous, and takes place in relatively pristine regions. In August and September, hundreds of active fires occur within a  $1^\circ \times 1^\circ$  grid cell, thus mimicking a spatially homogeneous source at the resolution of the model. This is a consequence of the limited time period during which ambient conditions favor burning in South America, and the concentration of agricultural development along the forest boundary.

At the beginning of the dry season in July, background  $\text{NO}_2$  concentrations are low. Thus, an increase in the  $\text{NO}_x$  concentration will decrease the  $\text{NO}_2$  lifetime. The instant dilution of the emissions will dampen this effect leading to an overestimation of the  $\text{NO}_2$  concentration in the model and an underestimation of  $\beta$ . For  $1^\circ \times 1^\circ$ , Valin et al. (2011) estimate the bias in the  $\text{NO}_2$  column is on the order of 25-50%, thus largely offsetting the low bias implied by the overestimated  $\text{NO}_2$  loss rate discussed above.

## 2.3 $\text{NO}_2$ Tropospheric Column Retrievals

Incorrect assumptions about the  $\text{NO}_2$  profile shape can lead to biases in the OMI air mass factor (AMF) used to convert tropospheric slant column densities to vertical column densities. The coarse resolution of the TM4 model that provides the a priori  $\text{NO}_2$  profile for the DOMINO retrieval may underestimate the surface level concentrations (Heckel et al., 2011). Recent work by (Bouscerez, 2013) shows the effect on the air mass factor of assuming an a priori  $\text{NO}_2$  profile without fire emissions. They find that AMFs would be biased low by as much as 50%, but on average 20-30%. This of course represents the upper limit for this bias, as the TM4 model a priori profiles do account for fire emissions. Therefore, a reasonable

estimate for this bias is 10-15% on average.

High aerosol loadings may also contribute to biases in NO<sub>2</sub> tropospheric columns retrieved from satellites (Leitão et al., 2010). If aerosols are well mixed with the NO<sub>2</sub> plume, enhanced light scattering will increase the sensitivity to NO<sub>2</sub> in this layer. AMFs would be underestimated and NO<sub>2</sub> tropospheric columns would be overestimated if this effect were not taken into account. If aerosols exist as a layer above the NO<sub>2</sub> plume, they effectively shield the lower atmosphere, reducing the sensitivity to NO<sub>2</sub>. Ignoring this effect would overestimate the AMFs and underestimate NO<sub>2</sub> tropospheric columns.

Observations from the Cloud-Aerosol Lidar with Orthogonal Polarization (CALIOP) instrument that has an overpass time within 15 minutes of OMI can provide some information regarding biomass burning aerosol layer heights over South America. However, CALIOP's narrow 335 m footprint does not allow for extrapolation of daily observations to biome scales. (Torres et al., 2013) developed a climatology of aerosol layer heights from 2.5 years of CALIOP observations, and found that they ranged from 2-4 km during the South American burning season. Individual orbital tracks show spatial heterogeneity of elevated and vertically well-mixed aerosol.

If we assume that a homogeneous elevated aerosol layer develops over the region in August and September, the peak burning months, shielding the surface emissions, OMI-DOMINO v2 NO<sub>2</sub> tropospheric columns could be underestimated by 50% (Lin et al., 2013). This number represents an upper limit, and is probably not representative of the typical aerosol induced retrieval error as some aerosol correction occurs via increased cloud fractions in the DOMINO retrieval (Boersma et al., 2011).

### 3 References

Deeter, M. N., Edwards, D. P., Gille, J. C. and Drummond, J. R.: Sensitivity of MOPITT observations to carbon monoxide in the lower troposphere, *Journal of Geophysical Research*, 112, D24306, doi:10.1029/2007JD008929, 2007.

Deeter, M. N., K, E. L., Edwards, D. P. and Gille, J. C.: Vertical resolution and information content of CO profiles retrieved by MOPITT, *Geophysical Research Letters*, 31, L15112,

doi:10.1029/2004GL020235, 2004.

Deeter, M. N., Martínez-Alonso, S., Edwards, D. P., Emmons, L. K., Gille, J. C., Worden, H. M., Pittman, J. V., Daube, B. C. and Wofsy, S. C.: Validation of MOPITT Version 5 thermal-infrared, near-infrared, and multispectral carbon monoxide profile retrievals for 2000–2011, *J. Geophys. Res. Atmos.*, n/a–n/a, doi:10.1002/jgrd.50272, 2013.

Deeter, M. N., Worden, H. M., Gille, J. C., Edwards, D. P., Mao, D. and Drummond, J. R.: MOPITT multispectral CO retrievals: Origins and effects of geophysical radiance errors, *Journal of Geophysical Research*, 116, D15303, doi:10.1029/2011JD015703, 2011.

Deeter, M., Edwards, D., Gille, J., Emmons, L. K., Francis, G., Ho, S. P., Mao, D., Masters, D., Worden, H. M., Drummond, J. R. and Novelli, P. C.: The MOPITT version 4 CO product: Algorithm enhancements, validation, and long-term stability, *Journal of Geophysical Research*, 115, D07306, 2010.

Kar, J., Jones, D. B. A., Drummond, J. R., Attié, J. L., Liu, J., Zou, J., Nichitiu, F., Seymour, M. D., Edwards, D. P., Deeter, M. N., Gille, J. C. and Richter, A.: Measurement of low-altitude CO over the Indian subcontinent by MOPITT, *Journal of Geophysical Research*, 113(D16), D16307, doi:10.1029/2007JD009362, 2008.

Rogers, C. D.: Inverse methods for atmospheric sounding: Theory and practice, World Scientific Publishing, 2000.

Worden, H. M., Deeter, M. N., Frankenberg, C., George, M., Nichitiu, F., Worden, J., Aben, I., Bowman, K. W., Clerbaux, C., Coheur, P. F., de Laat, A. T. J., Detweiler, R., Drummond, J. R., Edwards, D. P., Gille, J. C., Hurtmans, D., Luo, M., Martínez-Alonso, S., Massie, S., Pfister, G. and Warner, J.: Decadal record of satellite carbon monoxide observations, *Atmospheric Chemistry and Physics*, 13, 837–850, doi:10.5194/acp-13-837-2013, 2013.

Yurganov, L., McMillan, W., Grechko, E. and Dzhola, A.: Analysis of global and regional CO burdens measured from space between 2000 and 2009 and validated by ground-based solar tracking spectrometers, *Atmospheric Chemistry and Physics*, 10(8), 3479–3494, 2010.

Boersma, K. F., Eskes, H. J., Dirksen, R. J., van der A, R. J., Veefkind, J. P., Stammes, P., Huijnen, V., Kleipool, Q. L., Sneep, M., Claas, J., Leitão, J., Richter, A., Zhou, Y. and Brunner, D.: An improved tropospheric NO<sub>2</sub> column retrieval algorithm for the Ozone Monitoring Instrument, *Atmospheric Measurement Techniques*, 4, 1905–1928, doi:10.5194/amt-4-1905-2011, 2011.

Bousserez, N.: Space-based retrieval of NO<sub>2</sub> over biomass burning regions: quantifying and reducing uncertainties, *Atmospheric Measurement Techniques Discussions*, 6, 6645–6684 [online] Available from: <http://www.atmos-meas-tech-discuss.net/6/6645/2013/amt-6-6645-2013.pdf>, 2013.

Henderson, B. H., Pinder, R. W., Crooks, J., Cohen, R. C., Carlton, A. G., Pye, H. O. T. and Vizuete, W.: Combining Bayesian methods and aircraft observations to constrain the HO<sub>2</sub> + NO<sub>2</sub> reaction rate, *Atmospheric Chemistry and Physics*, 12(2), 653–667, doi:10.5194/acp-12-653-2012, 2012.

Heckel, A., Kim, S. W., Frost, G. J., Richter, A., Trainer, M. and Burrows, J. P.: Influence of low spatial resolution a priori data on tropospheric NO<sub>2</sub> satellite retrievals, *Atmospheric Measurement Techniques*, 4(9), 1805–1820, doi:10.5194/amt-4-1805-2011, 2011.

Leitão, J., Richter, A. and Vrekoussis, M.: On the improvement of NO<sub>2</sub> satellite retrievals—aerosol impact on the airmass factors, *Atmospheric Measurement Techniques*, 2010.

Lin, J. T., Martin, R. V., Boersma, K. F., Sneep, M., Stammes, P., Spurr, R., Wang, P., van Roozendael, M., Clémer, K. and Irie, H.: Retrieving tropospheric nitrogen dioxide over China from the Ozone Monitoring Instrument: effects of aerosols, surface reflectance anisotropy and vertical profile of nitrogen dioxide, *Atmos. Chem. Phys. Discuss.*, 13(8), 21203–21257, doi:10.5194/acpd-13-21203-2013, 2013.

Mollner, A. K., Valluvadasan, S., Feng, L., Sprague, M. K., Okumura, M., Milligan, D. B., Bloss, W. J., Sander, S. P., Martien, P. T., Harley, R. A., McCoy, A. B. and Carter, W. P. L.: Rate of Gas Phase Association of Hydroxyl Radical and Nitrogen Dioxide, *Science*, 330(6004), 646–649, doi:10.1126/science.1193030, 2010.

Stavrakou, T., Müller, J. F., Boersma, K. F., van der A, R. J., Kurokawa, J., Ohara, T. and Zhang, L.: Key chemical NO<sub>x</sub> sink uncertainties and how they influence top-down emissions of nitrogen oxides, *Atmospheric Chemistry and Physics*, 13, 9057–9082, doi:10.5194/acp-13-9057-2013, 2013.

Torres, O., Ahn, C. and Chen, Z.: Improvements to the OMI near-UV aerosol algorithm using A-train CALIOP and AIRS observations, *Atmospheric Measurement Techniques*, 6(11), 3257–3270, doi:10.5194/amt-6-3257-2013, 2013.

Valin, L. C., Russell, A. R., Hudman, R. C. and Cohen, R. C.: Effects of model resolution on the interpretation of satellite NO<sub>2</sub> observations, *Atmospheric Chemistry and Physics*, 11(22), 11647–11655, doi:10.5194/acp-11-11647-2011, 2011.

Vinken, G. C. M., Boersma, K. F., Jacob, D. J. and Meijer, E. W.: Accounting for non-linear chemistry of ship plumes in the GEOS-Chem global chemistry transport model, *Atmospheric Chemistry and Physics*, 11(22), 11707–11722, doi:10.5194/acp-11-11707-2011, 2011.

Williams, J. E., Strunk, A., Huijnen, V. and van Weele, M.: The application of the Modified Band Approach for the calculation of on-line photodissociation rate constants in TM5: implications for oxidative capacity, *Geoscientific Model Development*, 5, 15–35, doi:10.5194/gmd-5-15-2012, 2012.

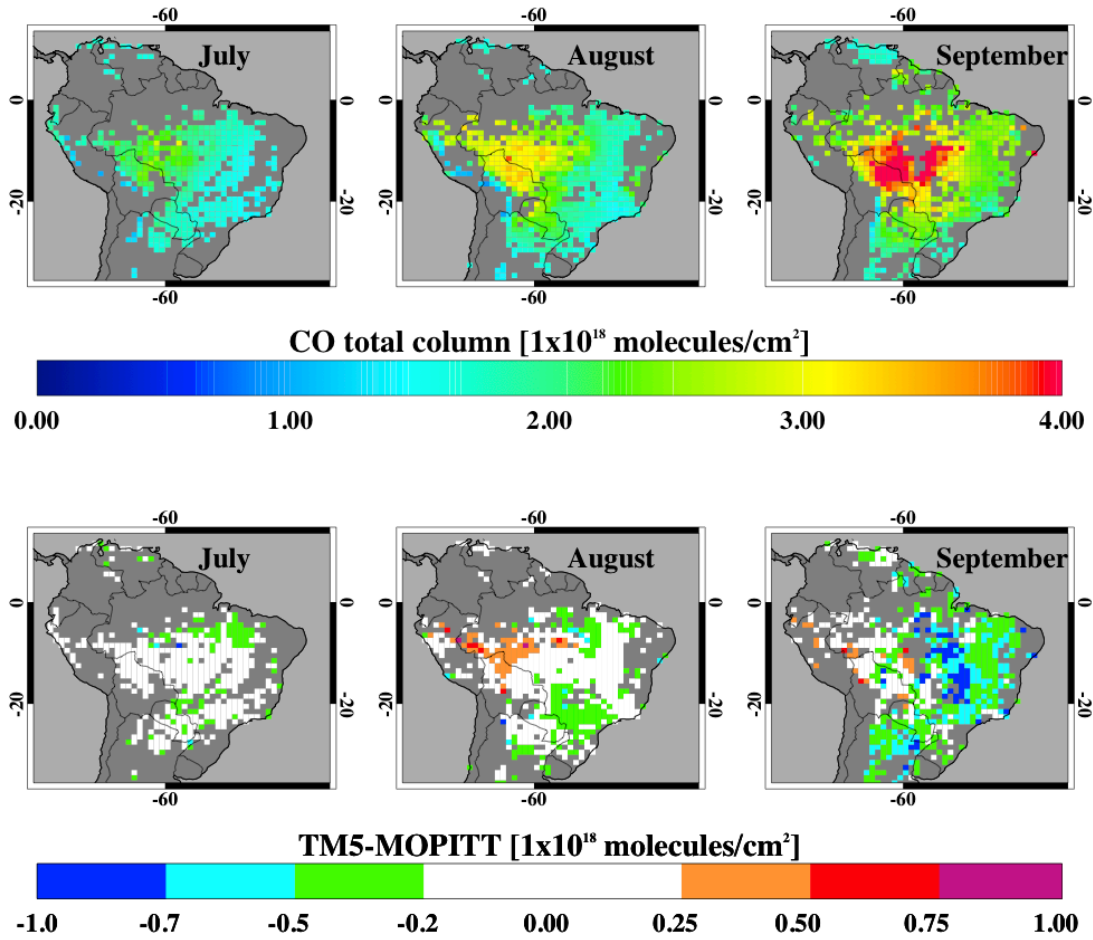


**Figure S1.** Comparison of monthly average MOPITT observed (top row) and TM5 simulated CO total columns. Only grid cells that have fire emissions as indicated by GFED v3 are considered in the monthly averages. Satellite observations were re-gridded to  $1^\circ \times 1^\circ$  on a daily basis, where grid cell averages were taken only when the satellite had enough valid observations to cover 30% of the grid cell. In the bottom row is the TM5 bias. Positive values indicate that the TM5 simulated CO total column is higher than the MOPITT observation. The simulated vertical profiles have been transformed with the MOPITT a priori profile and averaging kernel according to the strategy described in Section 3.

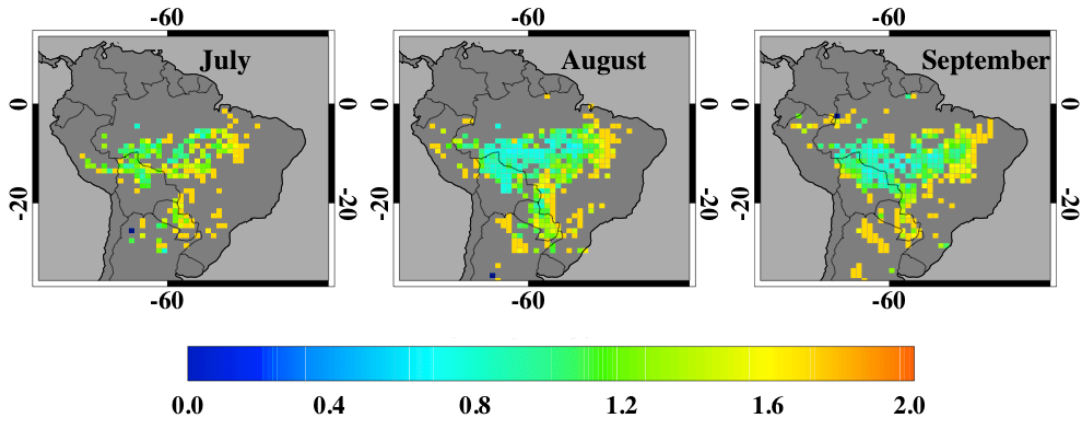


**Figure S2.** Monthly  $\beta$  sensitivity values (Eq. 2) calculated with the approach described in section 4. We only consider grid cells where fire  $\text{NO}_x$  emissions dominate over other emission sectors. Briefly, we calculate the change in TM5 modeled  $\text{NO}_2$  tropospheric columns after increasing the bottom up fire  $\text{NO}_x$  emissions by 15%. From these  $\text{NO}_2$  tropospheric column changes, we calculated daily  $\beta$  values that were then averaged to monthly values if multiple days of burning occur in a grid cell

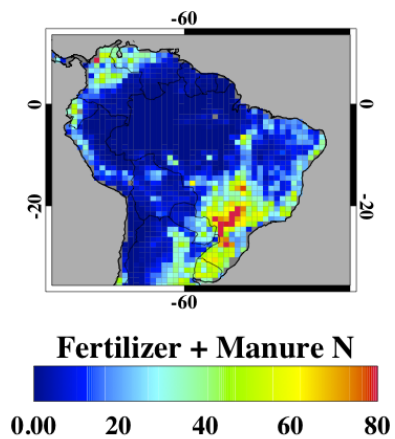


**Figure S3.** Fertilizer and manure nitrogen availability from Potter et al. (2010); units are kg/ha.

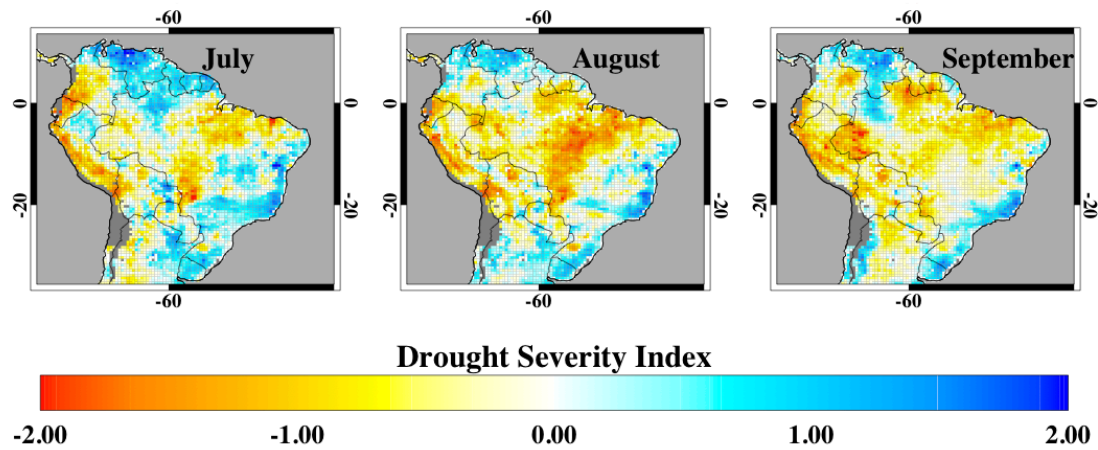


**Figure S4.** Drought severity index (DSI). Values less than zero indicate drier than normal conditions, and values greater than zero indicate wetter than normal conditions.